Journal of Physics: Conference Series

SERS analysis of Ag nanostructures produced by ion-beam deposition

IOP Conf. Series: Journal of Physics: Conf. Series **992** (2018) 012050 doi:10.1088/1742-6596/992/1/012050

SERS analysis of Ag nanostructures produced by ion-beam deposition

P A Atanasov[1,4] , N N Nedyalkov[1], Ru G Nikov[1], Ch Grüner[2], B Rauschenbach[2] and N Fukata[3]

[1]Emil Djakov Institute of Electronics, Bulgarian Academy of Sciences, 72 Tzarigradsko Chaussee, 1784 Sofia, Bulgaria
[2]Leibniz Institute of Surface Modification (IOM), Permoserstrasse 15, D-04318 Leipzig, Germany
[3]International Center for Materials for NanoArchitectonics (MANA), National Institute for Materials Science (NIMS), 1-1Namiki, Tsukuba 305-0044, Japan

E-mail: paatanas@hotmail.com

Abstract. This study deals with the development of a novel technique for formation of advanced Ag nanostructures (NSs) to be applied to high-resolution analyses based on surface enhanced Raman scattering (SERS). It has direct bearing on human health and food quality, e.g., monitoring small amount or traces of pollutants or undesirable additives. Three types of nanostructured Ag samples were produced using ion-beam deposition at glancing angle (GLAD) on quartz. All fabricated structures were covered with BI-58 pesticide (dimethoate) or Rhodamine 6G (R6G) for testing their potential for use as substrates for (SERS).

1. Introduction

The properties of noble metallic nanostructures (NSs) have been the subject of considerable fundamental and technological interest. Metal nanoparticles (NPs) play an important role in scientific research and nanotechnology. The interest in nanoscience and nanotechnologies has grown dramatically – the number of the various objects of nano research and applications has increased exponentially during the last decade [1]; the nanosystems find nowadays application in many areas, such as chemistry, optics, biology, medicine, microelectronics, etc.

The excitation spectrum of a given noble metallic sub-wavelength structure is determined by its surface plasmon resonances. The energies of plasmon resonances depend strongly on the shape and composition of the nanostructures. The tunability of the plasmon resonances of noble metallic NPs can be exploited to position the optical resonances at specific wavelength regions of interest and has led to a wide range of applications. The strong local electromagnetic field enhancement arising at a surface plasmon resonance has also been used to manipulate light-matter interactions, and noble metallic sub-wavelength structures have widely been applied to SERS [2,3]. The enhancement of the Raman signal may reach factors of up to 10^8-10^{12}, so that the method has been applied to detection of even single molecules [2]. The enhancement of the Raman signal is a result of the local enhancement of the

[4] To whom any correspondence should be addressed.

electromagnetic field in the vicinity of a structured surface due to the excitation of local and surface plasmons. In addition to their fundamental importance, plasmonic nanostructures have received a great deal of attention for potential applications in areas such as sub-wavelength waveguides, optical nanoantennas, photovoltaic technology for efficient light coupling into solar cells, metamaterials, chemical and biological sensing, and biomedicine [4-7].

Three-dimensional (3D) sculptured thin films (STF's) are truly nanostructured inorganic materials with anisotropic properties. They show a potential of being designed in a controllable manner using physical vapor deposition methods (PVD) for potentially multifunctional materials and products. Glancing angle ion-beam deposition (GLAD) is a sophisticated method of creating 3D chiral NSs with a tailored geometry. GLAD is based on controlling the self-shadowing between the growing crystallites/nanostructures. The self-organized nanostructure growth is based on a concurrent growth mechanism due to geometrical shadowing in combination with kinetic limitation for surface adatoms [8-10]. This technique requires a particle flux reaching the substrate under an extremely oblique angle of incidence (typically $\theta \sim 80$ deg). The growth conditions support a columnar growth, and the samples consist of 3D needles, which are slanted into the direction of the particle flux. The instantaneous change of the growth direction due to a simple variation of the incident vapor flux (by substrate rotation) allows for the fabrication of 3D nanostructures with manifold morphologies. Since the growth process is mainly determined by the shadowing length and the surface diffusion length, materials ranging from insulators to metals to semiconductors can be grown with 3D morphologies like spirals, chevrons, screws, pillars, needles etc. [11].

Chiral nanostructures are of particular interest due to their theoretically-predicted optical properties; uses have been proposed for such materials, e.g., as circularly-polarized light filters, in close similarity to liquid crystals [12]; or as sensors, filling liquids or gaseous substances into the open and porous structure of a sculptured thin film.

Zhou et al. [13] reported detection of polychlorinated biphenyls in soil and distilled spirit samples by surface-enhanced Raman scattering using Ag nanorod arrays as substrates produced by a glancing-angle e-beam technique. They detected polychlorinated biphenyls to a concentration of 5 μg/g in dry soil samples within one minute. Based on simulation, trace amounts were identified of an analyte in acetone solutions at a concentration of 10^{-6} mol/L.

Au or Ag NSs produced by laser methods were applied successfully to SERS. Thus, enhanced Raman spectrum has been observed of Rhodamine 6G (R6G) on Au nanocolumns created by off-axis PLD. R6G concentration as low as 1 nM [3] was measured and a maximum enhancement exceeding 10^5 was achieved.

SERS has been used for trace analyses of residues of different organophosphorous pesticides and insecticides [14-19]. Various nanostructures have been tested as substrates for the SERS analyses: solution of 100 nm Ag nanocubes [15], standard Klarite Au-coated SERS-active substrate [16-18]. The performance of SERS analyses has been compared with that of traditional analyses, such as chromatography, fluorescence polarization immunoassay, multi-enzyme inhibition assay, and biosensors. Although these methods can be used to detect trace amounts of pesticides, they are time consuming, labor-intensive, and expensive, making these analytical approaches less attractive and limiting laboratory, real-time, and field detections to some extent [16]. Among the large variety of pesticides, dimethoate is a very widely studied substance. The lowest concentration detected so far has been $5 \div 10$ $\mu g \cdot mL^{-1}$ using confocal Raman micro-spectrometry with Klarite substrates [16]. Generally, low concentration levels of about 10^{-6} have been reached.

This paper describes a study and the results of the development of a novel technology – CLAD ion-beam deposition – for formation of advanced Ag nanostructures (NSs) on quartz, which were applied to high-resolution analysis (SERS) of the BI-58 insecticide (dimethoate) and R6G as probing agents. The technology has direct bearing on human health and food quality, e.g., monitoring small amount or traces of pollutants or undesirable additives.

2. Experimental

A set of ion-beam deposited at glancing angle (GLAD) Ag NSs on quartz samples was prepared under different conditions (angle of incidence of the flow with respect to the substrate and rotation speed of the substrate).

The as prepared samples, to be used for SERS analyses, were covered by an aqueous solution of 0.2 % (800 μg/mL, i.e. 3.49 mM) of the insecticide with trade name BI-58 (containing dimethoate - $C_5H_{12}NO_3PS_2$), or an alcohol solution of 200 nM of R6G, and then were dried. The organophosphate insecticide dimethoate (commercially known as BI-58 – BASF SE, Ge) is one of the most widely used such agents. This compound is a basic substance at different concentration in a large number of insecticides used for treating plants. The standard colloid concentration of dimethoate in marketed BI-58 is 400 g/L (400 mg/mL). For plants treatment, it is diluted in water at a concentration of 0.2 %, i.e. 800 μg/ml. It is important to note that BI-58 consists of 37,4 % (W/W) dimethoate, 4,7 % (W/W) xylene and 48,4 % (W/W) cyclohexanone. The latter two compounds are solvents; when drops of BI-58 diluted in water were deposited on the surface of the substrates for analyses, they evaporated and disappeared during drying. Further, 200 nM R6G was used in order to check the sensitivity of the ion-beam deposited samples.

Table 1 presents a summary of the produced and analyzed samples. Samples **A** were covered by BI-58 (dimethoate), and $\mathbf{A_1}$, with R6G; θ is the glancing angle, the rotation speed is given in revolutions per minute (rpm).

Table 1. Summary description of the samples ion-beam-deposited at glancing angle and analyzed.

Samples A	**Ag NSs**	**3 samples:**	**Covered by 0.2% dimethoate – 3.49 mM**
		01a	400 nm; θ = 78°; normal thickness 1.5 μm; rotation speed 10 rpm
		01b	420 nm; θ = 78°; normal thickness 1.5μm; rotation speed 0 rpm
		01c	480 nm; θ = 86°; normal thickness: 2.5μm; rotation speed: 0 rpm
Samples A_1	**Ag NSs**	**3 samples:** 01a'; 01b'; 01c'	**Same as samples A, covered by 200 nM R6G**

The morphology of the samples was observed by scanning electron microscopy using a FE-SEM (Zeiss Ultra55, Gemini) microscope. The Raman spectra were obtained by an RMS-310 μ-Raman spectrometer (Photon Design, Japan). It uses a laser excitation power of 1 mW for detecting dimethoate and 0.0001 mW for detecting R6G, respectively, at a wavelength of λ = 532 nm and with a resolution of 0.2 cm^{-1}. The image dimension of the exciting laser beam on the surface of the checked substance is ~1 μm^2. It is worth noting that such a low excitation power was used to get the SERS spectra since the analytes are very sensitive to heating and are damaged even at very low excitation power.

3. Results and discussions

The morphology of the Ag nanostructures GLAD ion-beam-deposited on quartz substrates is presented in figure 1. As is seen, the structural properties are quite different and depend strongly on the deposition conditions.

All structures prepared were analyzed by μ-Raman spectrometry. SERS peaks of dimethoate appeared in all cases of structures deposited by the GLAD technology. Figure 2 a) is the Raman spectrum of dimethoate at the highest concentration (1.7 M), as purchased from an agriculture store,

and is given for reference. Figure 2 b) and c) present two parts of the spectrum detected from the structure shown in figure 1 a). Furthermore, figure 2 d) is a SERS spectrum of dimethoate taken from the Ag NSs presented in figure 1 c). The parameters of the SERS peaks originating from the Ag NSs, and the Raman peaks recorded from the highest dimethoate concentration are summarized in table 2.

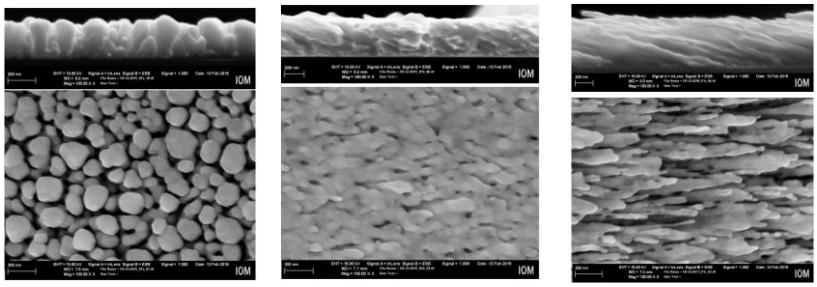

(a) (b) (c)

Figure 1. SEM images of Ag nanostructures deposited on quartz. **a)** film 400 nm (thickness of the structure at normal incidence 1.5 μm), θ = 78°, rotation 10 rpm; **b)** film 420 nm (thickness of the structure at normal incidence 1.5 μm), θ = 78°, rotation 0 rpm; **c)** film 480 nm (thickness of the structure at normal incidence 2.5 μm), θ = 86°, rotation 0 rpm.

Table 2. Summary of some important vibration modes observed (in cm^{-1}) of dimethoate. Relative intensity: vs – very strong; s – strong; m – middle; w – weak; vw – very weak; and br - broad. The results according to Ref. [16] are given for comparison and assignments of the vibrations; ν, δ and r denote stretching, deformation and torsion.

SERS peaks of 01a, 3.49 mM	SERS peaks of 01c, 3.49 mM	Raman peaks, 1.7 M	Ref. [16]			
			Peaks		Assignments	
			Raman	SERS	Raman	SERS
409, m	411, m	409, w	407	401	δ(P-O-C)	δ(P-O-C)
502, vs	503, vs	498, m	498	497	$r(CH_3)$	$r(CH_3)_v$
656, vs	656, w	656, vs	650	650	ν(P=S)	ν(P=S)
749, vs	750, vwbr	749, w				
	771, vs	773, vs				
	853, w	853, m				
1164, vs	1164, vs	1156, vw	1166	1160-1165	ν(C-C)	ν(C-C)
1276, s	1276, s	1266, w				
1417, m	1417, m	1417, wbr				
		1450, wbr	1449	1450	ν(O=C-N)I	ν(O=C-N)II
1520, vs						

The strongest peaks in the SERS of BI-58 (figure 2) are at 502, 656 and 1164 cm^{-1}, related according to Liu et al. [16] to CH_3 torsion, P=S stretching and C-C stretching vibrational modes, respectively. However, two other very strong peaks at 749 and 1520 cm^{-1} are also observed. According to Liu et al [17], the characteristic peaks of dimethoate are located at 494, 651 and 1640 cm^{-1}. The shallow peak (figure 2 c) at 1628 cm^{-1} can be assigned to the symmetric C=O stretching mode.We should note here that the slight differences between the peaks' positions in the μ-Raman and SERS spectra were recorded in our experiments with BI-58, when those reported in Refs. 16 and 17 were obtained from pure dimethoate.

In order to check the sensitivity of the ion-beam-produced structures for SERS analysis; 100 nM R6G was used. Figure 3 a) and b) show parts of the μ-Raman spectra of R6G produced by the samples presented in figure a) and c). The well-expressed peaks at 612 and 774 cm^{-1} are typical for this analyte [20]. Additionally, the intensities of the peaks taken using substrate 1 b (figure 1 c) are the highest, which is probably because of the needle structure (figure 1 c).

In what concerns the SERS sensitivity, the Ag NSs shown in figure 1 a and c exhibited the best properties. This is probably due to the character of these 3D structures – needle-like, which presents "hot spots" on their surfaces.

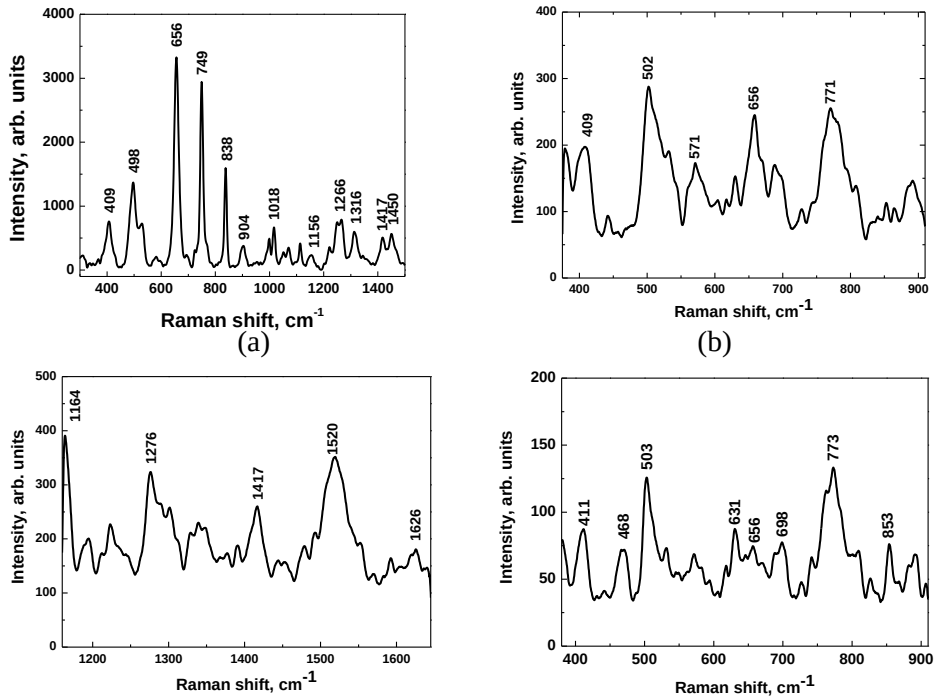

Figure 2. μ-Raman spectra of BI-58 a) at standard colloid concentration (400 mg/ml) for reference; b) and c) parts of SERS spectra of BI-58 deposited on Ag NSs which corresponds to the structure 01a in figure 1 a); d) for the structure 01c in figure 1 c). Excitation power was 1 mW.

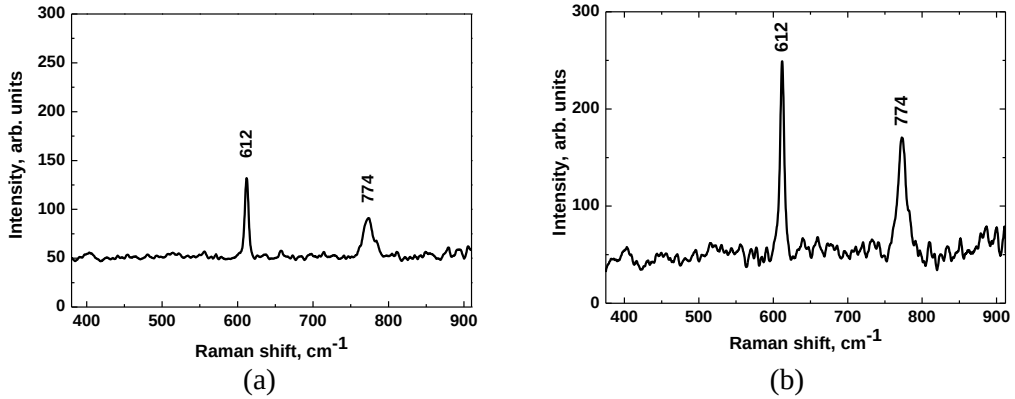

Figure 3. Parts of the μ-Raman spectra of R6G produced by the samples: a) **01a** (0.0001 mW, 20 s) and b) **01b** (0.0001 mW, 20 s).

4. Conclusions

Ion-beam deposition at glancing angle was used to form advanced Ag nanostructures (NSs) on quartz. They were applied to high-resolution analyses (SERS) of insecticide BI-58 (dimethoate) and R6G as probing agents. The lowest concentrations of the analytes studied using Ag NSs were 3.49 mM for BI-58 and 100 nM for R6G. This advanced technique of generating active substrates for SERS was

thus proven to be very attractive and useful for high-resolution analyses of different analytes. However, further improvement of the properties of the ion-beam-deposited at glancing angle structures is needed in order to achieve a higher resolution.

Acknowledgements
The work was supported in part under projects DNTS 01/1 and TO 2/24 funded by the Bulgarian National Science Fund. P. Atanasov highly acknowledges the financial support of JSPS under contract JSPS Fellow ID No. S16152.

References
[1] Bajpai S K and Yallapu M M eds 2009 *Recent Advances in Nanoscience and Technology* (Bentham Sci. Pub.)
[2] Nie S and Emory S R 1997 *Science* **275** 1102
[3] Sakano T, Tanaka Y, Nishimura R, Nedyalkov N N, Atanasov P A, Saiki T and Obara M 2008 *J. Phys.* D*: Appl. Phys*. **41**/23 235304
[4] Pissuwan D, Valenzuela S M and Cortie M 2006 *Trends Biotechnol*. **24**/2 62
[5] Huang X, El-Sayed I H, Qian W and El-Sayed M A 2006 *J. Am. Chem. Soc*. **128** 2115
[6] Cho W J, Kim Y and Kim Y K 2012 *ACS Nano* **6**/1 249
[7] Beliatis M J, Henley S J and Silva S R P 2011 *Opt. Lett.* **36** 1362
[8] Robbie K, Brett M J and Lakhtakia A 1995 *J. Vac. Sci. Technol.* A **13** 2991
[9] Smy T, Dew S K and Joshi R V J 2001 *Vac. Sci. Technol.* A **19**/1 251
[10] Robbie K, Beydaghyan G, Brown T, Dean C, Adams J and Buzea C 2004 *Rev. Sci. Instrum.* **74** 1089
[11] Patzig C, Rauschenbach B, Fuhrmann B and Leipner H J 2008 *J. Appl. Phys.* **103**/2 024313
[12] Robbie K, Broer D J and Brett M J 1999 *Nature* **399** 764
[13] Zhou Q, Zhang X, Huang Yu, Li Z and Zhang Z 2011 *Sensors* **11** 10851
[14] Guerrini L, Sanchez-Cortes S, Cruz V L, Martinez S, Ristori S and Feis A 2011 *J. Raman Spectrosc.* **42**/5 980
[15] Costa J, Ando R, Sant'Ana A and Corio P 2012 *Phys. Chem. Chem. Phys.* **14**/45 15645
[16] Liu Y, Ye B, Wan C, Hao Y, Lan Y and Ouyang A 2013 *Am. Soc. of Agricultural and Biological Eng.* **56**/3 1043
[17] Liu Y and Liu T 2011 *Int. Feder. for Inform. Processing AICT* **347** 427
[18] Bin L, Peng Z, Xiaoming L, Xin S, Hao L, Mengshi L 2013 *Food Bioprocess Technol.* **6** 710
[19] Zhang P X, Xiaofang Z, Andrew Y S, Cheng Y F 2006 *J. Phys.: Conf. Series* **28** 7
[20] Imamova S, Nedyalkov N, Dikovska A, Atanasov P, Sawczak M, Jendrzejewski R, Śliwiński G and Obara M 2010 *Appl. Surf. Sci.* **257**/3 1075